Research Article

The Journal of Comparative Neurology
Research in Systems Neuroscience
DOI 10.1002/cne.22804

Title

Bilateral connectivity in the brainstem respiratory networks of lampreys

Authors

Jean-François Gariépy[1], Kianoush Missaghi[1], Shannon Chartré[2], Maxime Robert[2], François Auclair[1] and Réjean Dubuc[1,2]

[1] Groupe de Recherche sur le Système Nerveux Central (GRSNC), Département de physiologie, Université de Montréal, Montréal, Québec, Canada.

[2] Groupe de Recherche en Activité Physique Adapté (GRAPA), Département de kinanthropologie, Université du Québec à Montréal, Montréal, Québec, Canada.

Abbreviated title

Brainstem respiratory networks in lampreys

Submitted to

Thomas E. Finger (Chemical Senses and Neurobiology of Anamniote Vertebrates)

Keywords

Respiration, neuroanatomy, retrograde labelling, anterograde labelling, bilateral, descending command, whole-cell patch recordings

Corresponding author

Dr Réjean Dubuc
Département de Kinésiologie
Université du Québec à Montréal
C.P. 8888 Succ. Centre-ville
Montréal (Québec), Canada, H3C 3P8
Tel: +1-514-343-5729
Fax: +1-514-343-6611
Email address: rejean.dubuc@gmail.com

Acknowledgments for support: This work was supported by grants to R.D. from the Natural Sciences and Engineering Research Council of Canada (NSERC, 217435), from the Canadian Institutes of Health Research (CIHR, 15129), from the Great Lake Fisheries Commission (GLFC, 8400272) and from the Fonds de la Recherche en Santé du Québec (FRSQ, group grant, 5249). J.-F.G. received studentships from the FRSQ and the Canadian Institutes of Health Research (CIHR, 84765). K.M. received studentships from NSERC and the FRSQ.

Received: Aug 10, 2011; Revised: Oct 19, 2011; Accepted: Oct 25, 2011

Abstract

This study examines the connectivity in the neural networks controlling respiration in lampreys, a basal vertebrate. Previous studies have shown that the lamprey paratrigeminal respiratory group (pTRG) plays a crucial role in the generation of respiration. Using a combination of anatomical and physiological techniques, we characterized the bilateral connections between the pTRGs and descending projections to the motoneurons. Tracers were injected in the respiratory motoneuron pools to identify pre-motor respiratory interneurons. Retrogradely labelled cell bodies were found in the pTRG on both sides. Whole-cell recordings of the retrogradely labelled pTRG neurons showed rhythmical excitatory currents in tune with respiratory motoneuron activity. This confirmed that they were related to respiration. Intracellular labelling of individual pTRG neurons revealed axonal branches to the contralateral pTRG and bilateral projections to the respiratory motoneuronal columns. Stimulation of the pTRG induced excitatory post-synaptic potentials (EPSPs) in ipsi- and contralateral respiratory motoneurons as well as in contralateral pTRG neurons. A Xylocaine injection on the midline at the rostro-caudal level of the pTRG diminished the contralateral motoneuronal EPSPs as well as a local injection of CNQX and AP-5 on the recorded respiratory motoneuron. Our data show that neurons in the pTRG send two sets of axonal projections: one to the contralateral pTRG and another to activate respiratory motoneurons on both sides through glutamatergic synapses.

Introduction

Respiration is a vital motor function controlled by neurons of the brainstem and spinal cord in vertebrates. Identifying the connections between the different respiratory regions is a focus of research in several animal models including fishes, amphibians and mammals. It has been argued that the respiratory oscillators from different classes of vertebrates could be homologous (Vasilakos et al., 2005; Wilson et al., 2006; Kinkead, 2009), but a better understanding of the neuronal networks underlying respiratory rhythmogenesis is needed for comparative analysis. This study focuses on the neural networks controlling respiration in the lamprey, a basal vertebrate.

In mammals, respiration is insured by the contraction of respiratory muscles that are activated by motoneurons located in the spinal cord and brainstem. The spinal cord contains motoneurons activating the diaphragm, the intercostal muscles and the abdominal muscles involved in breathing (Dobbins and Feldman, 1994; Giraudin et al., 2008). The brainstem contains motoneurons activating muscles of the upper respiratory pathways through the facial (VII), glossopharyngeal (IX), vagal (X), and hypoglossal (XII) nerves (Hwang et al., 1988; Bianchi and Pásaro, 1997). In lampreys, all respiratory motoneurons are located in the motor nuclei of the VII, IX and X cranial nerves (Rovainen, 1977; Guimond et al., 2003), none being located in the spinal cord (Martel et al., 2007).

In this study, we investigated the bilateral projections of neurons in the respiratory generator as well as their descending projections to the respiratory

motoneurons in lampreys. In mammals, the neural areas that generate the respiratory pattern have been explored in several studies. These areas are located in the brainstem and include the preBötzinger complex (preBötC), the retrotrapezoid nucleus/parafacial respiratory group (RTN/pFRG) and the Kölliker-Fuse nucleus (Smith et al., 1991; Onimaru and Homma, 2003; Del Negro et al., 2005; Feldman and Janczewski, 2006; Janczewski and Feldman, 2006; Onimaru and Homma, 2006; Barnes et al., 2007; Pace et al., 2007; Del Negro et al., 2008; Rubin et al., 2009; Abdala et al., 2009; Mörschel and Dutschmann, 2009; Feldman, 2010; Pagliardini et al., 2011). Anatomical studies have revealed abundant interconnections between these areas as well as with other areas of the brainstem involved in the neural control of respiration, including the caudal and rostral ventral respiratory groups and the Bötzinger complex (Smith et al., 1989; Tan et al., 2010).

Researchers have also identified crossing connections between the brainstem respiratory centers (Onimaru et al., 1993; Bouvier et al., 2010; Tan et al., 2010) and some were shown to play a crucial role for synchronizing the respiratory rhythm on both sides (Bouvier et al., 2010). The ventral respiratory group and the Bötzinger complex also send efferent projections to the brainstem and spinal cord areas that contain respiratory motoneurons and some of these connections cross and might participate in the bilateral synchronization of the respiratory rhythm (Feldman et al., 1985; Ellenberger and Feldman, 1988; Janczewski and Karczewski, 1990; Goshgarian et al., 1991; Dobbins and

Feldman, 1994; Alheid et al., 2002; Ezure et al., 2003; Li et al., 2003; Duffin and Li, 2006; Tarras-Wahlberg and Rekling, 2009).

The studies performed in mammals have revealed some of the interconnections between the brainstem respiratory areas. However, an understanding of the interactions between the properties of single neurons and their connectivity will likely be obtained from preparations in which the recording of single neurons is made possible while preserving the entire central respiratory network intact. Some of the important questions that remain relate to the extent of the role of individual neurons in the network. For instance, could individual neurons send crossing connections as well as project to the respiratory motononeurons, or are there separate neuronal populations with each type of projections? We have addressed this question using the brainstem preparation of lamprey.

A region of the rostro-lateral rhombencephalon, the paratrigeminal respiratory group (pTRG), has been identified as necessary for respiratory rhythmogenesis in lampreys (Kawasaki, 1979; Thompson, 1985; Martel et al., 2007; Mutolo et al., 2007; Mutolo et al., 2010). In this study, we have identified a population of pTRG neurons sending projections to the brainstem motor nuclei involved in breathing using retrograde labelling. In addition, single-cell recording and labelling allowed us to confirm that these pTRG neurons were related to respiration and that they sent axonal branches to both the respiratory motoneurons and the contralateral pTRG. Some of the implications of these results with regards to the evolution of the neural systems controlling breathing in

vertebrates are discussed.

Materials and methods

Experiments were performed on 57 post-metamorphic and adult sea lampreys, *Petromyzon marinus,* that were collected from the Great Chazy river (NY, USA), from Lake Huron (ON, CAN), and from Morpion Stream (Ste-Sabine, QC, CAN). The animals were kept in aerated water at 7 °C. All surgical and experimental procedures conformed to the guidelines of the Canadian Council on Animal Care and were approved by the Animal Care and Use Committee of the Université de Montréal and the Université du Québec à Montréal. Care was taken to minimize the number of animals used and their suffering.

Anatomical experiments

The connections between the pTRG of both sides of the brain and the descending connections from the pTRG to the respiratory motoneurons were examined using the tracers biocytin (Sigma) and Texas-Red dextran amines (3000 MW, Invitrogen/Molecular probes). Animals were first deeply anesthetised with MS-222 (Sigma, 100 mg/l in fresh water) and their brainstem was completely isolated *in vitro*, with the exception of the underlying cranium that was kept for pinning and support. During the dissection and the experiments, the preparations were kept at 7-9°C in continuously-renewed oxygenated Ringer's of the following composition (in mM): NaCl, 130; KCl, 2.1; CaCl2, 2.6; MgCl2, 1.8; HEPES, 4; dextrose, 4; NaHCO3, 1. The pH was adjusted to 7.4 with NaOH. The brain tissue at the site of tracer injection was first lesioned under visual guidance with

the tip of a glass micropipette to allow the local neuronal processes to pick up the tracer (Glover et al., 1986). Crystals of tracers were inserted to dissolve in the lesioned area. To label the motoneurons, the VII, IX and X nerves were cut peripherally and crystals of tracer were deposited on the cut end of the nerves. The preparations were kept overnight in Ringer's to allow tracers to be transported. They were then fixed in 4% paraformaldehyde in phosphate buffered saline (PBS: 0.1 M, pH 7.4 with 0.9% NaCl) for 24 hours at 4°C, transferred to 20% sucrose in phosphate buffer (0.1 M, pH 7.4) for cryoprotection, and cut transversally or parasagittally in a cryostat (25 µm thickness). The sections were collected on ColorFrost Plus slides (Fisher Scientific) and left to dry on a warming plate at 37°C overnight. The next day, the sections were either mounted directly with Vectashield (Vector Laboratories) or incubated as follows to reveal the biocytin: three 10 min rinses with PBS, 60 min incubation in streptavidin conjugated to Alexa Fluor 488 (Invitrogen) diluted 1:200 in PBS at room temperature, three rinses with PBS, a quick rinse in distilled H_2O, and air drying for 15 min. These slides were then mounted with Vectashield. The size of the retrogradely labelled pTRG neurons was measured with a 40X objective and a micrometric scale incorporated in the ocular of the fluorescence microscope. Only neurons with a clearly visible nucleus were measured along their longest axis. To provide a general idea of the range of neuronal diameters, we sampled 101 pTRG neurons in 3 animals.

Electrophysiological experiments

The animals were anesthetised and dissected similarly to anatomical experiments. The brainstem preparation was pinned down onto silicone elastomer (Sylgard) at the bottom of an experimental chamber continually perfused with cold Ringer's at a rate of ~4 ml/min.

Extracellular recordings of respiratory motoneurons were made using glass electrodes filled with Ringer's and placed on the surface of the X nucleus (tip diameter ≈ 5 µm). The electrodes were connected to an AC amplifier (Model 1800, A-M Systems; low cut-off: 100 Hz; high cut-off: 500 Hz). Respiratory motoneurons were recorded intracellularly with sharp glass microelectrodes (4 M KAc; 80 -120 MΩ). The signals were amplified by an Axoclamp 2A amplifier (Axon Instruments, Foster City, CA; sampling rate: 10 kHz). The motoneurons were impaled by directing the tip of the electrode to the IX / rostral X motor nuclei. In some experiments, the pTRG was electrically stimulated with single pulses (1 to 10 µA) using glass-coated tungsten microelectrodes (0.8–2 MΩ) at a rate of 0.05 Hz.

To determine the localization of the descending pathways from the pTRG to respiratory motoneurons, injections of Xylocaine (2%, AstraZeneca, Mississauga, ON, Canada) were made with a micropipette using a Picospritzer (General Valve, Fairfield, NJ). In some experiments, the glutamatergic receptor blockers 6-cyano-7-nitroquinoxaline-2,3-dione (CNQX, 1mM) and (2R)-amino-5-phosphonovaleric acid (AP-5, 500 µM) were injected on intracellularly recorded respiratory motoneurons. In all cases, the inactive dye, Fast Green, was added to the drug solution to monitor the size and exact location of the injections. The size

of the injections was estimated visually to be no more than 300 µm in diameter. The duration of pressure injections was adapted to the flow of the drug solution out of the micropipette, varying from several seconds to minutes.

Whole-cell recordings from pTRG neurons were also performed to characterize the activity of pTRG neurons and their projections in the brainstem. As a first step, Texas-Red dextran amines were injected in the X nucleus *in vivo* to retrogradely label the pTRG neurons to be recorded the following day. A 2 mm^2 opening was made on the top of the cranium to expose the caudal brainstem of the anesthetised animal. The tracers were introduced in the X nucleus and the incision was then closed with Vetbond (3M Animal Care Products, St-Paul, MN). The animal was then returned to a small nursery aquarium filled with oxygenated Ringer's solution for the night at room temperature and an *in vitro* isolated brainstem preparation was performed as described above on the following day. In order to access the pTRG cells with patch electrodes, part of the dorsal hindbrain was removed using a vibratome. The alar plate lateral to the V motor nucleus, the dorsal part of the V motor nucleus, the dorsal isthmic region and the optic tectum were removed. The cells were targeted under an Eclipse FN-1 microscope (Nikon Instruments) equipped for fluorescence. The patch solution contained (mM): cesium methane sulfonate 102.5, NaCl 1, $MgCl_2$ 1, EGTA 5, HEPES 5 and 0.1% biocytin for intracellular labelling of the entire axonal arborization of the recorded cell. The pH was adjusted to 7.2 with CsOH and pipettes were pulled to a tip resistance of 5 MΩ.

Patch recordings were made in whole-cell voltage-clamp mode (-70 mV) with a Model 2400 amplifier (A-M Systems).

Data acquisition and analyses

Data were acquired via a Digidata 1322A interface using Clampex 9 software (Axon Instruments) for computer analysis. Excitatory post-synaptic potentials (EPSPs) were analysed using Spike2 version 5.19 (Cambridge Electronic Design) and homemade scripts. Averages from 20 to 100 EPSPs per animals were used for comparing control, effect, and washout conditions.

Data in the text and figures are given as means ± standard deviation. Statistical analyses were carried out using SigmaStat v3.5 (Systat Software). A Student's *t*-test was used to compare the means of two groups. A Mann-Whitney test was used when the compared distributions did not respect the assumptions of normality of distribution or equality of variance. Repeated measures ANOVA were used when comparing more than two groups. Distributions were considered statistically significant when the value of *P* was lower than 0.05.

The sections were observed and photographed with an E600 epifluorescence microscope equipped with a DXM1200 digital camera (Nikon Canada) using FITC or Texas-Red filter sets. The figures were designed and assembled using CorelDraw X4 (Corel) and Illustrator CS4 (Adobe) software. Photoshop CS4 software (Adobe) was used to make small adjustments when merging photomicrographs taken with separate fluorescence filter sets. All purely

red-green images were transferred to magenta-green in Photoshop to make our work accessible to those who have red-green color blindness.

The axonal projections of each injected neuron were analyzed in detail using fluorescence microscopy. A 3D reconstruction was made from one typical pTRG neuron for illustrative purposes using Neurolucida (MBF Neuroscience). In addition to the contours of the brainstem, the MRRN, PRRN, V, VII, IX, X motor nuclei, and the pTRG were also outlined based on the location of the cell bodies in each nucleus.

Results

Anatomical tracing experiments

Neuronal tracers were injected in the pTRG, the respiratory motoneuronal pools, and the respiratory nerves in order to identify the connections between the pTRGs on both sides and their descending projections to respiratory motoneurons. A first series of experiments was undertaken to retrogradely label the pTRG neurons that project to respiratory motoneurons by injecting tracers unilaterally in the respiratory motoneuronal pools (Fig. 1A) (n = 21). In a subset of these experiments, an additional injection of fluorescent dextran amines or biocytin in the ipsilateral (n = 6) or contralateral (n = 6) pTRG areas in order to identify putative crossing projections between the pTRGs of both sides of the brain.

Neurons in the pTRG were labelled from unilateral motoneuronal injections. A population of large cells (cell bodies from 25 to 40 µm) was labelled in the pTRG, close to the medial and dorsal borders of the trigeminal sensory root (rdV) (Figs. 1B-F, 2D, E). These neurons were found both ipsilaterally and contralaterally to the motoneuronal injection (Fig. 2). They had at least one very large dendrite that arborized within the rdV (Fig. 1E, F), and a very conspicuous axon that crossed the midline at the level of the cell body (Fig. 1B). Smaller cells were also found more dorsally in the ipsilateral and contralateral pTRG (Figs. 1E, green and white cells). These neurons were located laterally to the V motor nucleus, close to the sulcus limitans. The cells were either round, bipolar, or

multipolar and the largest diameter of their soma varied from 10 to 23 μm (hydrated tissue).

The additional injection in the pTRG also labelled many small to medium-size neurons (10 to 23 μm) in the contralateral pTRG area (Fig. 1C, D; magenta and blue dots in the pTRG area in Fig. 2D, E). Some larger and more ventrolaterally located cells were also labelled. These cells were very similar to the ones described above after injections in the motor nucleus (Fig. 1C, blue arrow). It is also worth noting that numerous labelled fibres crossed the midline. Some of these fibres were likely anterogradely labelled as they displayed many varicosities in the contralateral pTRG area and seemed to terminate amongst the cell bodies retrogradely labelled from the motoneuronal injection (Fig. 1D). Double-labelled neurons (neurons that were labelled by the pTRG and the motoneuronal injections) were found in the pTRG whether the injected pTRG was located ipsilaterally or contralaterally to the injected motoneuronal pool (Fig. 1E, F, open arrow; blue dots in pTRG area in Fig. 2D, E). These results suggest that single cells in the pTRG could send projections to both the pTRG on the opposite side and to the respiratory motoneuronal column.

Another series of anatomical experiments was designed to reveal the anterograde projections from the pTRG area to the respiratory motoneurons (Fig. 3A) (n = 3). Biocytin was injected on the proximal stump of the cut nerves VII, IX and X on both sides. Respiratory motoneurons were intensively labelled as seen on parasagittal sections (magenta cells, Fig. 3B). The apical dendrites of the motoneurons arborized heavily in the subependymal layer (sep in Fig. 3),

whereas their basal dendrites extended ventrally and also arborized heavily in an area close to the ventrolateral border of the tegmentum (Fig. 3B). In the same preparations, FITC-conjugated dextran amines were injected into the pTRG area on one side only, to visualize the descending projections from the pTRG (Fig. 3, green). The majority of the fibres arising from the pTRG area were seen ipsilateral to this injection, with a very similar but smaller distribution on the contralateral side (Fig. 3C2, D2). A large number of fibres coursed longitudinally within the subependymal layer (Fig. 3B, C2), and varicosities were seen close to the apical dendrites of the respiratory motoneurons (Fig. 3C). Other fibres, some of larger calibre, coursed longitudinally in the tegmentum ventral to the motoneurons, close to the motoneurons' basal dendrites (Fig. 3B, especially clear to the right of the photograph due to the angle of the section relative to the distribution of the motor nuclei as seen in A). These ventral fibres had fewer varicosities, but some were in close proximity to the motoneurons' basal dendrites (Fig. 3C2, D2). Some anterogradely labelled fibres entered the cell body layer of the motoneuron populations (Fig. 3B, C2, C4, D2, D3). Overall, the anatomical experiments support the hypothesis that some pTRG neurons project directly to the contralateral pTRG and to the respiratory motoneuronal nuclei.

Electrophysiological characterization of the descending pTRG projections

To further characterize the bilateral descending projections from the pTRG to the respiratory motoneurons, individual respiratory motoneurons were

recorded intracellularly, while stimulating the pTRG on both sides. Increasing stimulation intensities (1-10 μA) were used until a maximal intensity was reached that just induced action potentials. This facilitated the quantitative analysis of the postsynaptic potentials (see Figs. 4 and 5). All of the recorded respiratory motoneurons displayed larger EPSPs in response to stimulation of both contralateral and ipsilateral pTRGs. The latency was generally longer for contralateral stimulation (10.2 ± 3.8 vs. 7.4 ± 4.0 ms; paired t-test; $P < 0.05$; n=4). The maximum slope of the response onset was slightly larger for contralateral stimulation (1.35 ± 0.57 vs. 1.07 ± 0.23 mV/ms; paired t-test; $P < 0.05$; n=4). The area of EPSPs varied from one preparation to another and the exact location of the stimulating electrodes in the pTRG. However, there was no significant difference between responses to contralateral and ipsilateral stimulation when pooling data from all preparations (176.9 ± 141.3 mV*ms contra; 233.7 ± 134.5 mV*ms ipsi; paired t-test; $P = 0.28$; n=4). Because the stimulating electrodes in the pTRG on each side may have been positioned at different locations in the pTRGs, paired intracellular recordings were made from a respiratory motoneuron on each side while stimulating the pTRG on one side (n=2) (Fig. 4). As in the previous experiment, the latency of the EPSPs was longer in the motoneuron contralateral to the stimulation (13.7 ± 3.1 vs 4.8 ± 0.6 ms; two-tailed t-test; $P < 0.001$; n=2). The EPSPs in both motoneurons followed high frequencies of stimulation with little attenuation (Fig. 4C-F, 10 to 40 Hz), suggesting a fast and efficient connection.

Localization of descending inputs from the pTRG to the respiratory motoneurons

In order to localize the trajectory of the crossing descending projections from the pTRG to respiratory motoneurons, Xylocaine was injected to block neural activity at different locations along the presumed axonal tract projection linking the pTRGs and the respiratory motoneurons (Fig. 5A). Some of the injections were made along the midline at the rostrocaudal level of the pTRG. These injections dramatically decreased the motoneuronal response to stimulation of the contralateral pTRG area (Fig. 5B) (EPSPs area reduction of 60.6 ± 22.5 %; One-way repeated measures ANOVA; $P < 0.05$; 7 cells, 7 preparations). After washout, the EPSPs recovered (Fig. 5B) (77.1 ± 27.9 % of control; One-way repeated measures ANOVA; $P > 0.05$). A Xylocaine injection made in the pTRG located ipsilaterally to the recorded respiratory motoneuron decreased the area of EPSPs elicited by stimulation of the contralateral pTRG (Fig. 5C) (47.0 ± 19.8 % reduction; One-way repeated measures ANOVA; $P < 0.05$; 5 cells, 5 preparations). After washout, the EPSPs recovered (Fig. 5C) (95.5 ± 49.7 % of control; One-way repeated measures ANOVA; $P > 0.05$). To determine if the reduction was due to an effect on synaptic connections between the two pTRGs or to blocking action potentials in axons travelling laterally in the contralateral pTRG before descending to motoneurons, CNQX and AP-5 were injected instead of Xylocaine. These injections also led to decreases in the area of EPSPs, suggesting that a synaptic relay was present (Fig. 5D) (59.5 ± 20.3 % reduction; One-way repeated measures ANOVA; $P < 0.05$; 4 cells, 4 preparations). After washout, the EPSPs did not recover (Fig. 5D) (40.6 ± 29.9 %

of control; One-way repeated measures ANOVA; $P < 0.05$). These results suggest that the pTRG of one side of the brain sends bilateral descending inputs to respiratory motoneurons and that a part of the crossing connection relays in the contralateral pTRG.

Effects of blocking ionotropic glutamatergic receptors on the recorded motoneurons

To identify the neurotransmitter responsible for the excitatory inputs from the pTRG to respiratory motoneurons, a mixture of CNQX/AP5 was injected over the IX and X motor nuclei. This abolished the respiratory bursts recorded extracellularly from the motoneurons. The effect on EPSPs elicited in respiratory motoneurons in response to the ipsi- or contralateral pTRG varied from a complete abolition to a large reduction (Fig. 5E) (70.2 ± 30.2 % reduction; One-way repeated measures ANOVA; $P < 0.05$; 7 cells; 7 preparations). The EPSPs recovered during the washout period (84.0 ± 24.7 % of control; One-way repeated measures ANOVA; $P > 0.05$).

Anatomical characterization of pTRG neurons at the single-cell level

Previous anatomical experiments allowed us to examine the projections at a population level. Because of the large number of labelled fibres, it is impossible to follow the course of the axonal projections from individual neurons. To

circumvent this problem, we patch recorded individual pTRG neurons and injected them intracellularly with biocytin (Fig. 6) (n = 8). To focus on the pTRG neurons projecting to respiratory motoneurons, Texas-Red dextran amines were injected in the X motor nucleus 24 hours before the electrophysiological experiment. The labelled neurons were then targeted under a fluorescence microscope for whole-cell patch recordings. Under voltage-clamp, these neurons displayed rhythmically-occurring inward currents that preceded the respiratory bursts recorded extracellularly from the motoneurons (Fig. 6A). To test electrophysiologically whether these neurons received inputs from the contralateral pTRG, electrical stimulation of the latter was performed (n = 3) and large inward currents were induced in the recorded pTRG neuron (Fig. 6B). After filling the recorded cells with biocytin, a relatively constant pattern of projections was observed. Table 1 shows the regions of the brainstem where each of the recorded neuron (n = 8) projected fibres with varicosities. Most neurons projected to the contralateral pTRG as well as bilaterally to the VII, IX and X respiratory motoneuron nuclei (Fig. 6C-G). Two neurons had unilateral projections on the ipsi- and contralateral side, respectively (Table 1). These results indicate that the pattern of projection of individual neurons in the paratrigeminal respiratory group (pTRG) is similar to that seen with population labelling: 6 out of 8 recorded neurons displayed projections to the contralateral respiratory-generating area and bilateral projections to the respiratory motoneuronal columns.

Discussion

This study shows that lamprey pTRG neurons possess a complex axonal arborization with projections to multiple brainstem sites involved in respiration. We identified three sets of projections from pTRG neurons: one set of projections to the contralateral pTRG, one to the ipsilateral respiratory motoneuronal column and one to the contralateral motoneuronal column. One of the most salient results in this study is that individually labelled pTRG neurons were shown to possess these three sets of projections. These findings are represented on a schematic of the lamprey brainstem (Fig. 7).

Bilateral connections

We found that neurons in the pTRG project to the contralateral pTRG. Furthermore, the electrophysiological experiments show that glutamatergic synapses in the contralateral pTRG are partly involved in the inputs to the contralateral respiratory motoneurons. This suggests that crossing glutamatergic connections at the pTRG level might influence the output of the respiratory generator to the respiratory motoneurons.

Xylocaine injections along the midline at the pTRG level had an even stronger effect than unilateral pTRG blockade. These injections almost completely abolished the EPSPs. One possible explanation for this is that the axons relaying the inputs to contralateral motoneurons cross the midline in a rather compact bundle. As they reach the other side the axons spread out with

some coursing down to project to respiratory motoneurons without reaching the contralateral pTRG. Other axonal projections would reach relay cells in the contralateral pTRG that in turn send their axons down to the respiratory motoneurons. This is consistent with the anatomical finding of a dense bundle of decussating axons at the midline that spreads out as it progresses laterally. Individually filled pTRG neurons also displayed separate axonal branches to the contralateral pTRG and bilateral projections to the respiratory motoneurons. The injections of Xylocaine in the pTRG might block one branch without blocking the descending branch that travels medially and projects to the motoneurons.

We have thus found anatomical and electrophysiological evidence for two sets of projections that might underlie the bilateral synchronization of respiratory activity: the decussating descending axons from the pTRG to the motoneurons of both sides and decussating axons to the contralateral pTRG. This is similar to what was found in mammals where contralateral projections exist between respiratory-generating regions (Bouvier et al., 2010; Tan et al., 2010) and from respiratory-generating regions to respiratory motoneurons (Janczewski and Karczewski, 1990; Goshgarian et al., 1991; Duffin and Li, 2006; Tarras-Wahlberg and Rekling, 2009). Some Bötzinger complex neurons were found to project both to the ipsilateral and contralateral brainstem (Ezure et al., 2003), but whether individual preBötC and pFRG neurons possess similar complex axonal arborizations remains to be determined. In our study, we found that most pTRG neurons possess projections both to the contralateral respiratory-generating area and the motoneuronal columns. Overall, 6 out of 8 individually-labelled cells

displayed the two types of projections. This proportion may be an underestimation as the vibratome might have cut a part of the axonal arborization for some of the labelled neurons.

The requirement for a strong coordination between the two sides of the brain is not exclusive to respiratory systems. For instance, in feeding systems, interneurons were found to synchronize bilaterally the networks underlying suckling in neonatal rats (Koizumi et al., 2009). Locomotor networks of the spinal cord also need bilateral coordination, with the particularity that this coordination is often in anti-phase (Fagerstedt et al., 2000; Grillner, 2003; Mentel et al., 2008; Brocard et al., 2010).

Descending projections

This study shows that pTRG neurons send axonal branches that travel caudally to the VII, IX and X nuclei. Previous studies have shown that gill contractions propagate rostro-caudally in lampreys (Guimond et al., 2003) in such a way that muscles of the seventh gill pore were activated with a slight delay compared to muscles of the first gill pore. The major part of that delay was attributed to the longer X nucleus axons compared to those of the VII nucleus, from the soma in the brainstem to their respective gill muscles. However, recordings over respiratory motoneuron cell bodies showed that there was still a delay of 5 ms between the rostral and caudal motoneuronal pools. This could not be attributed to axon length, and the rostro-caudal course of axons originating

from the pTRG neurons characterized in the present study might be responsible. A similar rostro-caudal delay was also observed between the respiratory motoneuronal pools of the spinal cord in rats (Giraudin et al., 2008). In the locomotor networks of the lamprey spinal cord, the spinal segments also display a rostro-caudal delay during forward locomotion. Ascending, descending, long, and short axonal projections as well as excitability gradients are at play (Cohen et al., 1992; Matsushima and Grillner, 1992; see also Kozlov et al., 2009). Whether some of these are involved in the respiratory rostro-caudal delay in lampreys remains to be determined.

We have shown that glutamate receptor blockers injected over respiratory motoneurons abolish their excitatory responses to pTRG stimulation. This indicates that connectivity between the pTRG and the brainstem respiratory motoneurons uses glutamate as a neurotransmitter. This is similar to mammals where both spinal and brainstem respiratory motoneurons are activated by excitatory glutamatergic synapses (Greer et al., 1991; Berger, 2000; Wang et al., 2002).

Comparative aspects relative to the brainstem respiratory networks in vertebrates

The localization of the pTRG pre-motor interneurons has important implications for understanding how the respiratory networks have evolved in vertebrates. The pTRG has been previously identified in lampreys by showing that chemical or physical lesion of this region abolishes breathing (Rovainen

1977; Kawasaki, 1979; Thompson, 1985; Martel et al., 2007; Mutolo et al., 2007; Mutolo et al., 2010). However, pTRG neurons had never been observed anatomically. Four hypotheses may be considered regarding the fate of the pTRG during evolution: 1) it is homologous to the lung oscillator of amphibians, which in turn would be homologous to the preBötC of mammals, 2) it is homologous to the the buccal oscillator of amphibians, which in turn would be homologous to the pFRG in mammals, 3) it is homologous to the medial parabrachial or Kölliker-Fuse nucleus, or 4) it was lost during evolution and was replaced by non-homologous networks. Because both the pFRG and the preBötC are located more caudally in the brainstem than the pTRG cells described in this study, the first two hypotheses would imply that the respiratory generator has been displaced from a rostral to a caudal position during evolution from the common ancestors of lampreys and other vertebrates to mammals. In support of the first hypothesis, some studies have shown similarities between the pTRG in lampreys, the lung oscillator in amphibians and the preBötC in mammals. For instance, opiate-sensitivity was shown in the pTRG in lampreys (Mutolo et al., 2007), the lung oscillator in amphibians (Vasilakos et al., 2005) and the preBötC in mammals (Gray et al., 1999). Furthermore, co-application of I_{NaP} and I_{CAN} current blockers (riluzole and flufenamic acid, respectively) in the pTRG of lampreys or the preBötC of rodents abolishes the respiratory rhythm. In both cases, the rhythm can be restarted by substance P (Del Negro et al., 2005; Mutolo et al., 2010). However, in support of the second hypothesis, the pTRG of lampreys is functionally closer to the gill oscillator of amphibians because it

produces gill movements. Finally, in support of the third hypothesis, the pTRG is located in the lateral pons, similarly to the medial parabrachial and Kölliker-Fuse nuclei. The respiratory regions of the pons are believed to play a role in phase-switching in mammals (Cohen, 1971; von Euler et al., 1976; Arata et al., 2010) while some argue that they are necessary to generate eupnea (St John, 2009). It is difficult to determine what happened to the pTRG of lampreys in evolution based solely on pharmacological and anatomical data. It was recently shown that the preBötC neurons are derived from a group of Dbx1-expressing progenitors (Gray et al., 2010) and further knowledge of the developmental origins of the pTRG neurons identified in this study might provide an answer. Nearby motor control structures such as the reticular nuclei and the mesencephalic locomotor region have been studied in several species and are thought to be homologous to corresponding mammalian structures (Cabelguen et al., 2003; Dubuc, 2009; Martin et al., 2011; Le Ray et al, 2011). It is thus likely that a better understanding of the respiratory-generating networks and their development in a wide range of species will allow us to address the question of homology between the respiratory oscillators in vertebrates.

Other Acknowledgments

We are very grateful to Danielle Veilleux for her technical assistance, to Christian Valiquette for his skilful programming of data analysis software, and to Frédéric Bernard for his help with the graphics and the figures. We thank Dr. Roger Bergstedt, William D. Swink, and Mary K. Jones from the Lake Huron Biological Station in Michigan, Brad Young and Wayne Bouffard from the U.S. Fish and Wildlife Service of Vermont, and R. McDonald from the Sea Lamprey Control Center in Sault Ste. Marie for their kind supply of lampreys.

References

Abdala AP, Rybak IA, Smith JC, Zoccal DB, Machado BH, St John WM, Paton JF. 2009. Multiple pontomedullary mechanisms of respiratory rhythmogenesis. Respir Physiol Neurobiol 168:19-25.

Alheid GF, Gray PA, Jiang MC, Feldman JL, McCrimmon DR. 2002. Parvalbumin in respiratory neurons of the ventrolateral medulla of the adult rat. J Neurocytol 31:693-717.

Arata A, Tanaka I, Fujii M, Ezure K. 2010. Active inspiratory-expiratory phase switching mechanism exists in the neonatal nucleus parabrachialis. Adv Exp Med Biol 669:135-138.

Barnes BJ, Tuong CM, Mellen NM. 2007. Functional imaging reveals respiratory network activity during hypoxic and opioid challenge in the neonate rat tilted sagittal slab preparation. J Neurophysiol 97:2283-2292.

Berger AJ. 2000. Determinants of respiratory motoneuron output. Respir Physiol 122:259-269.

Bianchi AL, Pásaro R. 1997. Organization of central respiratory neurons. In: Miller AD, Bianchi AL, Bishop BP, editors. Neural control of the respiratory muscles. CRC Press, Florida, USA.

Bouvier J, Thoby-Brisson M, Renier N, Dubreuil V, Ericson J, Champagnat J, Pierani A, Chédotal A, Fortin G. 2010. Hindbrain interneurons and axon guidance signaling critical for breathing. Nat Neurosci 13:1066-1074.

Brocard F, Ryczko D, Fénelon K, Hatem R, Gonzales D, Auclair F, Dubuc R. 2010. The transformation of a unilateral locomotor command into a symmetrical bilateral activation in the brainstem. J Neurosci 30:523-533.

Cabelguen JM, Bourcier-Lucas C, Dubuc R. 2003. Bimodal locomotion elicited by electrical stimulation of the midbrain in the salamander Notophthalmus viridescens. J Neurosci 23:2434-2439.

Cohen MI. 1971. Switching of the respiratory phases and evoked phrenic responses produced by rostral pontine electrical stimulation. J Physiol 217:133-158.

Cohen AH, Ermentrout GB, Kiemel T, Kopell N, Sigvardt KA, Williams TL. (1992) Modelling of intersegmental coordination in the lamprey central pattern generator for locomotion. Trends Neurosci 15:434-438.

Del Negro CA, Morgado-Valle C, Hayes JA, Mackay DD, Pace RW, Crowder EA, Feldman JL. 2005. Sodium and calcium current-mediated pacemaker neurons and respiratory rhythm generation. J Neurosci 25:446-453.

Del Negro CA, Pace RW, Hayes JA. 2008. What role do pacemakers play in the generation of respiratory rhythm? Adv Exp Med Biol 605:88-93.

Dobbins EG, Feldman JL. 1994. Brainstem network controlling descending drive to phrenic motoneurons in rat. J Comp Neurol 347:64-86.

Dubuc R. 2009. Locomotor regions in the midbrain (MLR) and diencephalon (DLR). In: Binder MD, Hirokawa N, Windhorst U, editors. The encyclopedia of neuroscience. Springer, New York, USA.

Duffin J, Li YM. 2006. Transmission of respiratory rhythm: midline-crossing connections at the level of the phrenic motor nucleus? Respir Physiol Neurobiol 153:139-147.

Ellenberger HH, Feldman JL. 1988. Monosynaptic transmission of respiratory drive to phrenic motoneurons from brainstem bulbospinal neurons in rats. J Comp Neurol 269:47-57.

Ezure K, Tanaka I, Saito Y. 2003. Brainstem and spinal projections of augmenting expiratory neurons in the rat. Neurosci Res 45:41-51.

Fagerstedt P, Zelenin PV, Deliagina TG, Orlovsky GN, Grillner S. 2000. Crossed reciprocal inhibition evoked by electrical stimulation of the lamprey spinal cord. Exp Brain Res 134:147-154.

Feldman JL. 2010. Looking forward to breathing. Prog Brain Res 188:213-218.

Feldman JL, Loewy AD, Speck DF. 1985. Projections from the ventral respiratory group to phrenic and intercostal motoneurons in cat: an autoradiographic study. J Neurosci 5:1993-2000.

Feldman JL, Janczewski WA. 2006. Counterpoint: The preBötC is the primary site of respiratory rhythm generation in the mammal. J Appl Physiol 100:2094-2098.

Giraudin A, Cabirol-Pol MJ, Simmers J, Morin D. 2008. Intercostal and abdominal respiratory motoneurons in the neonatal rat spinal cord: spatiotemporal organization and responses to limb afferent stimulation. J Neurophysiol 99:2626-2640.

Glover JC, Petursdottir G, Jansen JK. 1986. Fluorescent dextran-amines used as axonal tracers in the nervous system of the chicken embryo. J Neurosci Methods 18:243-254.

Goshgarian HG, Ellenberger HH, Feldman JL. 1991. Decussation of bulbospinal respiratory axons at the level of the phrenic nuclei in adult rats: a possible substrate for the crossed phrenic phenomenon. Exp Neurol 111:135-139.

Gray PA, Hayes JA, Ling GY, Llona I, Tupal S, Picardo MC, Ross SE, Hirata T, Corbin JG, Eugenín J, Del Negro CA. 2010. Developmental origin of preBötzinger complex respiratory neurons. J Neurosci 30:14883-14895.

Gray PA, Rekling JC, Bocchiaro CM, Feldman JL. 1999. Modulation of respiratory frequency by peptidergic input to rhythmogenic neurons in the preBötzinger complex. Science 286:1566-1568.

Greer JJ, Smith JC, Feldman JL. 1991. Role of excitatory amino acids in the generation and transmission of respiratory drive in neonatal rat. J Physiol 437:727-749.

Grillner S. 2003. The motor infrastructure: from ion channels to neural networks. Nat Rev Neurosci 4:573-586.

Guimond JC, Auclair F, Lund JP, Dubuc R. 2003. Anatomical and physiological study of respiratory motor innervation in lampreys. Neuroscience 122:259-266.

Hwang JC, Chien CT, St John WM. 1988. Characterization of respiratory-related activity of the facial nerve. Respir Physiol 73:175-187.

Janczewski WA, Karczewski WA. 1990. The role of neural connections crossed at the cervical level in determining rhythm and amplitude of respiration in cats and rabbits. Respir Physiol 79:163-175.

Janczewski WA, Feldman JL. 2006. Distinct rhythm generators for inspiration and expiration in the juvenile rat. J Physiol 570:407-420.

Kawasaki R. 1979. Breathing rhythm-generation in the adult lamprey, Entosphenus japonicus. Jpn J Physiol 29:327-338.

Kinkead R. 2009. Phylogenetic trends in respiratory rhythmogenesis: Insights from ectothermic vertebrates. Respir Physiol Neurobiol 168:39-48.

Koizumi H, Nomura K, Yokota Y, Enomoto A, Yamanishi T, Lida S, Ishihama K, Kogo M. 2009. Regulation of trigeminal respiratory motor activity in the brainstem. J Dent Res 88:1048-1053.

Kozlov A, Huss M, Lansner A, Kotaleski JH, Grillner S. 2009. Simple cellular and network control principles govern complex patterns of motor behavior. Proc Natl Acad Sci U S A 106:20027-20032.

Le Ray D, Juvin L, Ryczko D, Dubuc R. 2011. Supraspinal control of locomotion: the mesencephalic locomotor region. Prog Brain Res 188:51-70.

Li YM, Shen L, Peever JH, Duffin J. 2003. Connections between respiratory neurones in the neonatal rat transverse medullary slice studied with cross-correlation. J Physiol 549:327-332.

Martel B, Guimond JC, Gariépy J-F, Gravel J, Auclair F, Kolta A, Lund JP, Dubuc R. 2007. Respiratory rhythms generated in the lamprey rhombencephalon. Neuroscience 148:279-293.

Martin E, Devidze N, Shelley D, Westberg L, Fontaine C, Pfaff D. 2011. Molecular and neuroanatomical characterization of single neurons in the mouse medullary gigantocellular reticular nucleus. J Comp Neurol 519:2574-2593.

Matsushima T, Grillner S. 1992. Neural mechanisms of intersegmental coordination in lamprey: local excitability changes modify the phase coupling along the spinal cord. J Neurophysiol 67:373-388.

Mentel T, Cangiano L, Grillner S, Büschges A. 2008. Neural substrates for state-dependent changes in coordination between motoneuron pools during fictive locomotion in the lamprey spinal cord. J Neurosci 28:868-879.

Mörschel M, Dutschmann M. 2009. Pontine respiratory activity involved in inspiratory/expiratory phase transition. Philos Trans R Soc Lond B Biol Sci 364:2517-2526.

Mutolo D, Bongianni F, Cinelli E, Pantaleo T. 2010. Role of neurokinin receptors and ionic mechanisms within the respiratory network of the lamprey. Neuroscience 169:1136-1149.

Mutolo D, Bongianni F, Einum J, Dubuc R, Pantaleo T. 2007. Opioid-induced depression in the lamprey respiratory network. Neuroscience 150:720-729.

Onimaru H, Kashiwagi M, Arata A, Homma I. 1993. Possible mutual excitatory couplings between inspiratory neurons in caudal ventrolateral medulla of brainstem-spinal cord preparation isolated from newborn rat. Neurosci Lett 150:203-206.

Onimaru H, Homma I. 2003. A novel functional neuron group for respiratory rhythm generation in the ventral medulla. J Neurosci 23:1478-1486.

Onimaru H, Homma I. 2006. Point: The pFRG is the primary site of respiratory rhythm generation in the mammal. J Appl Physiol 100:2094-2098.

Pace RW, Mackay DD, Feldman JL, Del Negro CA. 2007. Inspiratory bursts in the preBötzinger complex depend on a calcium-activated non-specific cation current linked to glutamate receptors in neonatal mice. J Physiol 582:113-125.

Pagliardini S, Janczewski WA, Tan W, Dickson CT, Deisseroth K, Feldman JL. 2011. Active expiration induced by excitation of ventral medulla in adult anesthetized rats. J Neurosci 31:2895-2905.

Rovainen CM. 1977. Neural control of ventilation in the lamprey. Fed Proc 36:2386-2389.

Rubin JE, Hayes JA, Mendenhall JL, Del Negro CA. 2009. Calcium-activated nonspecific cation current and synaptic depression promote network-dependent burst oscillations. Proc Natl Acad Sci U S A 106:2939-2944.

Smith JC, Morrison DE, Ellenberger HH, Otto MR, Feldman JL. 1989. Brainstem projections to the major respiratory neuron populations in the medulla of the cat. J Comp Neurol 281:69-96.

Smith JC, Ellenberger HH, Ballanyi K, Richter DW, Feldman JL. 1991. Pre-Botzinger complex: a brainstem region that may generate respiratory rhythm in mammals. Science 254:726-729.

St John WM. 2009. Noeud vital for breathing in the brainstem: gasping--yes, eupnoea--doubtful. Philos Trans R Soc Lond B Biol Sci 364:2625-2633.

Tan W, Pagliardini S, Yang P, Janczewski WA, Feldman JL. 2010. Projections of preBötzinger complex neurons in adult rats. J Comp Neurol 518:1862-1878.

Tarras-Wahlberg S, Rekling JC. 2009. Hypoglossal motoneurons in newborn mice receive respiratory drive from both sides of the medulla. Neuroscience 161:259-268.

Thompson KJ. 1985. Organization of inputs to motoneurons during fictive respiration in the isolated lamprey brain. J Comp Physiol A 157:291-302.

Vasilakos K, Wilson RJ, Kimura N, Remmers JE. 2005. Ancient gill and lung oscillators may generate the respiratory rhythm of frogs and rats. J Neurobiol 62:369-385.

von Euler C, Marttila I, Remmers JE, Trippenbach T. 1976. Effects of lesions in the parabrachial nucleus on the mechanisms for central and reflex termination of inspiration in the cat. Acta Physiol Scand 96:324-337.

Wang J, Irnaten M, Venkatesan P, Evans C, Baxi S, Mendelowitz D. 2002. Synaptic activation of hypoglossal respiratory motorneurons during inspiration in rats. Acta Physiol Scand 3:195-199.

Wilson RJ, Vasilakos K, Remmers JE. 2006. Phylogeny of vertebrate respiratory rhythm generators: the Oscillator Homology Hypothesis. Respir Physiol Neurobiol 154:47-60.

Figure Legends

Figure 1: Morphology and location of neurons in the pTRG that project to the contralateral pTRG, the contralateral respiratory motoneuron pool, or both. A: Schematic representation of a dorsal view of the brain of the adult sea lamprey illustrating injection sites in the pTRG (magenta) and respiratory motoneurons (green). B: Photomicrograph of a cross section illustrating retrogradely labelled neurons (arrows) in the pTRG area after an injection of biocytin in the contralateral respiratory motoneuron pool. A population of large neurons with remarkable dendritic extensions was located in the contralateral pTRG and had a characteristic large-diameter axon that crossed the midline at the level of the cell body. Smaller cells were also present lateral to the trigeminal motor nucleus (V) and close to the sulcus limitans (sl). C: Photomicrograph of a cross section at the level of the anterior octavomotor nucleus (NOMA). A population of small cells (white arrows), located close to the sulcus limitans (sl), was labelled after tracer injections in the contralateral pTRG. A number of large rdV cells, similar to those described in B were also labelled (blue arrow). D: Higher power photomicrograph of pTRG neurons labelled after an injection in the contralateral pTRG. Note the presence of numerous anterogradely labelled, varicose fibres. E-F: Higher power photomicrographs of the contralateral pTRG area, in animals that received pTRG (magenta) and respiratory motoneuron (green) tracer injections on the same side. In the contralateral pTRG, double-labelled neurons (open arrows) were consistently found (E-F). Many neurons were also single-labelled (filled arrows).

In D-F, the midline is also to the left. The scale bar in A represents 2 mm. B-F: 100 µm.

Figure 2: Distribution of retrogradely labelled neurons in the pTRG area after tracer injections in the pTRG and in the respiratory motoneurons. A: Schematized representation of a dorsal view of the rhombencephalon where the levels of the cross sections in D and E are indicated. Line 1 passes through the level of the injection in the motor nucleus, whereas lines 2 to 4 pass through the level of the pTRG. B-C: Photomicrographs illustrating examples of injection sites with Texas-Red dextran amines (B, converted to magenta, see Materials and Methods) and biocytin (C, revealed with green streptavidin-Alexa Fluor 488, C). The area where the neural tissue was damaged by the injection pipette is delineated by a black line. D-E: Schematized cross sections from two typical preparations that received motoneuron and pTRG injections on opposite sides (D) or on the same side (E). The retrogradely labelled neurons shown on each illustrated section were sampled from three adjacent sections and pooled together into one. One section was skipped between each sampled section, to make sure that no cell was counted twice. This inevitably leads to an underestimation of the number of cells, but their distribution was the main interest. Double-labelled neurons appear in blue. The grayed areas around the injection sites represent regions where analysis was impossible due to the high intensity of fluorescence (see B, C). The areas filled with green or magenta correspond to the area where the tissue was damaged by the pipette. Rectangles

refer to the location of photomicrographs in B and C, and in Figure 1. The scale bars in B and C represent 200 µm. The scale bars in D and E represent 500 µm.

Figure 3: Projections from the pTRG area to respiratory motoneurons. A: Schematic representation of a dorsal view of the brain of the adult sea lamprey. To the right, the enlarged rhombencephalic region shows the location of the trigeminal (V), facial (VII), glossopharyngeal (IX) and vagal (X) motor nuclei at the bottom of the IVth ventricle. B: Photomicrograph of a parasagittal section through the respiratory motoneuron populations in a preparation that received a unilateral injection of FITC-dextran amines (green) into the pTRG. The motoneurons were labelled with biocytin (revealed in red with streptavidin-Alexa Fluor 594; displayed here in magenta) by injections of the three respiratory nerves peripherally. The illustrated section comes from the same side as the pTRG injection. Fibres from the pTRG area run longitudinally in the subependymal layer (sep) and in the tegmentum, ventral to the cell bodies of the motoneurons. Some of the fibres turn ventrally or dorsally to enter the motoneuron layer. C-D: High-power photomicrographs of glossopharyngeal respiratory motoneurons as they appear on cross sections. C1, D1: Motoneurons were clearly labelled on both sides of the brain (ipsi, ipsilateral, and contra, contralateral to the pTRG injection). Note the arborization of apical dendrites in the subependymal layer and basal dendrites in the tegmentum. C2, D2: Superimposed photomicrographs illustrating the proximity of fibres descending from the pTRG (green) and the dendrites and cell bodies of motoneurons.

Elements in white are not double-labelled but result from the superimposition of the varicosities labelled from the pTRG that are in close proximity to the respiratory motoneurons. C3, C4, D3: The boxed area in C2 and D2 were enlarged to better show the green varicosities around motoneuronal elements. The scale bar in A represents 2 mm. B, 200 µm. C1, C2, D1, D2, 50 µm. C3, 5 µm. C4, D3, 10 µm. Pro: Prosencephalon, Mes: Mesencephalon, Rh: Rhombencephalon, V:Trigeminal motor nucleus, VII: Facial motor nucleus, IX: Glossopharyngeal motor nucleus, X: Vagal motor nucleus.

Figure 4: Characterization of bilateral descending inputs from the pTRG to pairs of simultaneously-recorded respiratory motoneurons on the two sides of the brainstem. A: Schematic representation of the lamprey brainstem. A respiratory motoneuron is recorded simultaneously from the two sides of the brain and a stimulating electrode is placed in the pTRG on one side. B: Recordings of spontaneous on-going fictive respiratory activity from a pair of motoneurons (MN) located on each side. The intracellularly-recorded respiratory bursts are in phase with those recorded extracellularly from the vagal motor nucleus (X). C-F: Intracellular excitatory responses to paired pulse stimulation with increasing frequency (C, D, E and F correspond to 10, 20, 30 and 40 Hz, respectively). pTRG: paratrigeminal respiratory group, MN: motoneuron, X: Vagal motor nucleus, ipsi: ipsilateral, contra: contralateral.

Figure 5: Electrophysiological characterization of the descending connections from the pTRG to the respiratory motoneurons. A: Schematic representation of the lamprey brainstem with the pTRG and respiratory motoneurons represented on both sides. B: Average of the EPSPs recorded from a respiratory motoneuron following electrical stimulation of the contralateral pTRG. Xylocaine was applied along the midline at the pTRG level. C: Average of the EPSPs recorded from a respiratory motoneuron following electrical stimulation of the contralateral pTRG. Xylocaine was applied in the ipsilateral pTRG. D: Average of the EPSPs recorded from a respiratory motoneuron following a stimulation of the contralateral pTRG. CNQX (1 mM) and AP-5 (500 µM) were applied in the ipsilateral pTRG. E: Intracellular recording of a respiratory motoneuron during stimulation of the ipsilateral pTRG. CNQX and AP-5 were injected directly over the recorded motoneuron. pTRG: paratrigeminal respiratory group, ipsi, i: ipsilateral, contra, c: contralateral.

Figure 6: Electrophysiological and anatomical characterization of pTRG neurons. A: Patch recording of a pTRG neuron in whole-cell voltage-clamp mode. The neuron displays inward currents in phase with the respiratory activity recorded extracellularly from the vagal motor nucleus (X). B: Average of the inward currents induced by electrical stimulation of the contralateral pTRG. C: Superimposition of three photomicrographs of the recorded pTRG neuron filled with biocytin (green) and retrogradely-filled from an injection of dextran

amines (red) in the X nucleus. DAPI labelling, in blue, shows the location of DNA-containing cell nuclei. D: 3D reconstruction of the axonal projections of the recorded pTRG neuron seen from a dorsal view of the rhombencephalon. Varicosities and dendritic spines are represented as circles. The diameter of the axons, dendrites and cell body (→) were amplified for better visibility. Dendrites, red arborizations; Soma, blue; Axons, yellow arborizations; V, red; VII, light blue; IX, light yellow; X, light gray; pTRG, purple. E: Photomicrograph illustrating axonal branches from the pTRG neuron innervating the ipsilateral facial motor nucleus (VII). F1: Photomicrograph illustrating axonal branches from the pTRG neuron around the dendrites of the IX nucleus. The outlined area corresponds to the photograph in F2. F2: Z-projection of 14 adjacent optic slices (0.5 µm each) obtained from a confocal microscope. A larger diameter axonal branch with no varicosity (green, left arrow) and a smaller diameter axonal branch with varicosities (green, right arrow) were located in close proximity to the basal dendrites of the IX motoneurons (magenta) labelled from the tracer injection in the adjacent motoneuron pool. *, blood vessel. G: Photomicrograph illustrating axonal branches from the pTRG neuron innervating the contralateral pTRG. → indicates axonal branches. The scale bar in C represents 100 µm. D, the three axes represent 500 µm. E, 50 µm. G, 100 µm. F1, 100 µm. F2, 10 µm.

Figure 7: Schematic representation of the newly-identified connectivity in the respiratory networks of lampreys. Our study shows that neurons in the

paratrigeminal respiratory group (pTRG), located in the rostral rhombencephalon, send axonal arborizations to the contralateral pTRG and bilaterally to the respiratory motoneurons. VII: facial nucleus, IX: glossopharyngeal nucleus, X: vagal nucleus.

Table 1: Summary of the projections from the recorded pTRG neurons. A checkmark indicates the presence of at least one branch containing varicosities in the structure or around the dendrites of the neurons located in the structure. pTRG: paratrigeminal respiratory group, VII: facial nucleus, IX: glossopharyngeal nucleus, X: vagal nucleus, i: ipsilateral, c: contralateral.

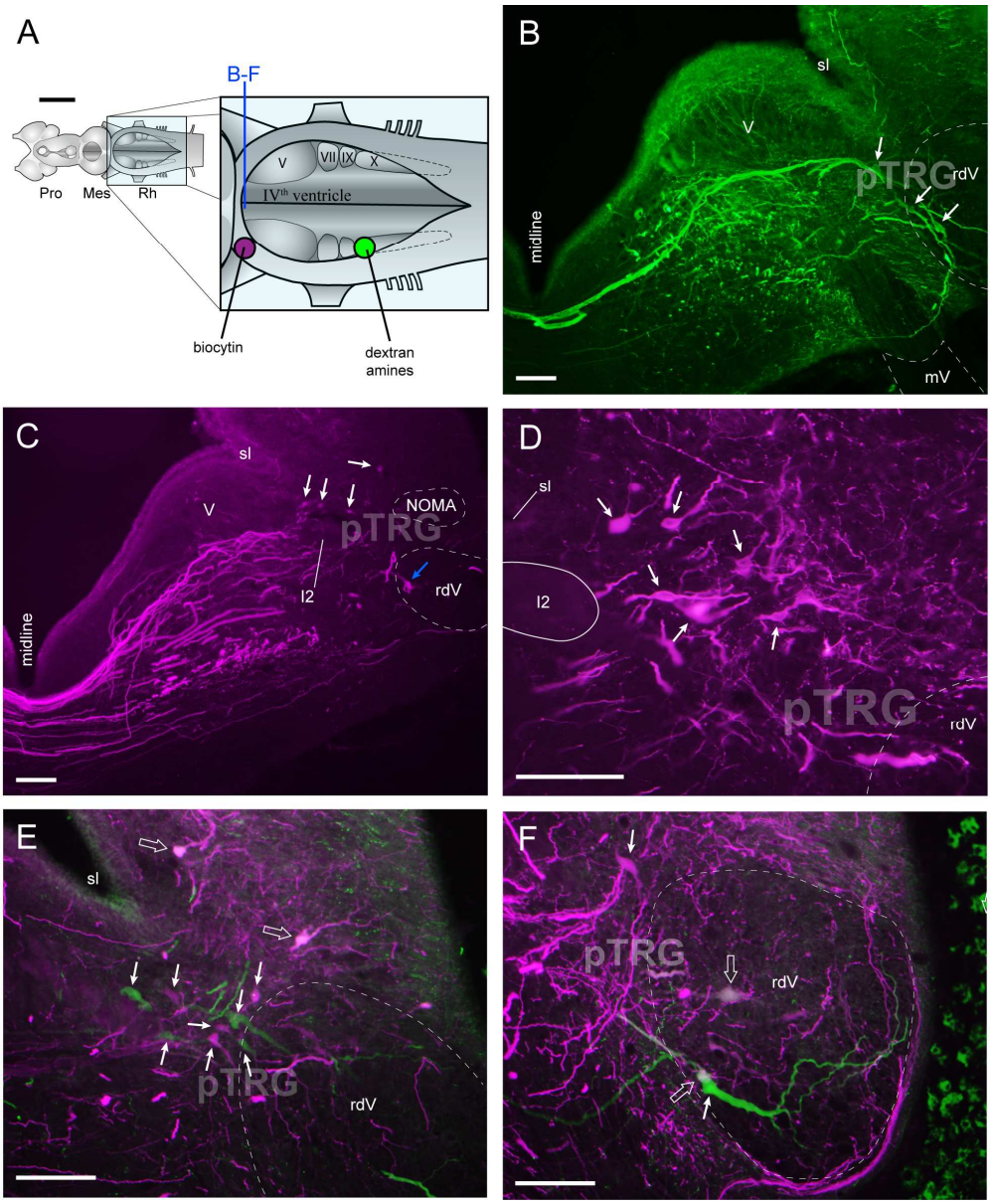

Morphology and location of neurons in the pTRG that project to the contralateral pTRG, the contralateral respiratory motoneuron pool, or both. A: Schematic representation of a dorsal view of the brain of the adult sea lamprey illustrating injection sites in the pTRG (magenta) and respiratory motoneurons (green). B: Photomicrograph of a cross section illustrating retrogradely labelled neurons (arrows) in the pTRG area after an injection of biocytin in the contralateral respiratory motoneuron pool. A population of large neurons with remarkable dendritic extensions was located in the contralateral pTRG and had a characteristic large-diameter axon that crossed the midline at the level of the cell body. Smaller cells were also present lateral to the trigeminal motor nucleus (V) and close to the sulcus limitans (sl). C: Photomicrograph of a cross section at the level of the anterior octavomotor nucleus (NOMA). A population of small cells (white arrows), located close to the sulcus limitans (sl), was labelled after tracer injections in the contralateral pTRG. A number of large rdV cells, similar to those described in B were also labelled (blue arrow). D: Higher power photomicrograph of pTRG neurons labelled after an injection in the contralateral pTRG. Note the

presence of numerous anterogradely labelled, varicose fibres. E-F: Higher power photomicrographs of the contralateral pTRG area, in animals that received pTRG (magenta) and respiratory motoneuron (green) tracer injections on the same side. In the contralateral pTRG, double-labelled neurons (open arrows) were consistently found (E-F). Many neurons were also single-labelled (filled arrows). In D-F, the midline is also to the left. The scale bar in A represents 2 mm. B-F: 100 μm.
165x199mm (300 x 300 DPI)

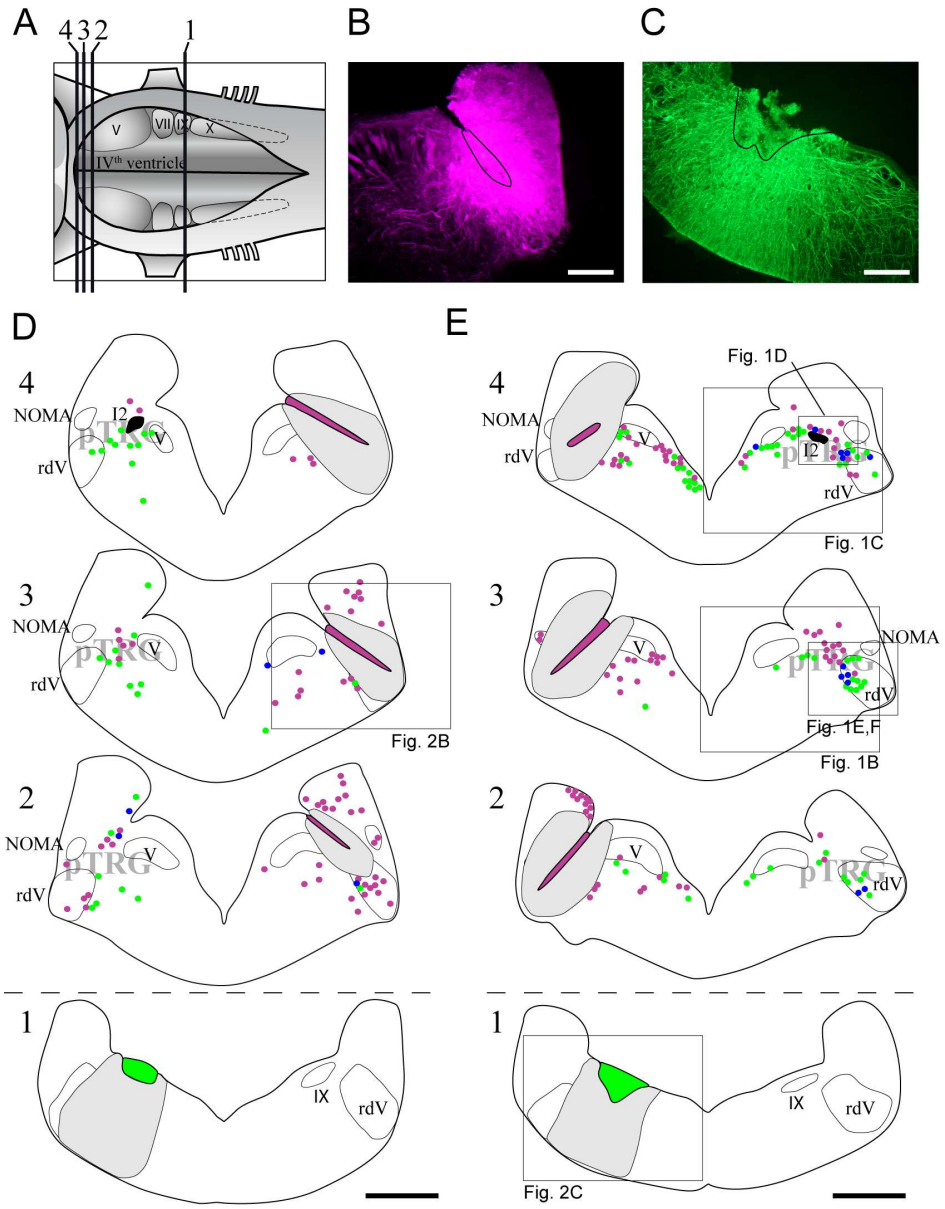

Distribution of retrogradely labelled neurons in the pTRG area after tracer injections in the pTRG and in the respiratory motoneurons. A: Schematized representation of a dorsal view of the rhombencephalon where the levels of the cross sections in D and E are indicated. Line 1 passes through the level of the injection in the motor nucleus, whereas lines 2 to 4 pass through the level of the pTRG. B-C: Photomicrographs illustrating examples of injection sites with Texas-Red dextran amines (B, converted to magenta, see Materials and Methods) and biocytin (revealed with green streptavidin-Alexa Fluor 488, C). The area where the neural tissue was damaged by the injection pipette is delineated by a black line. D-E: Schematized cross sections from two typical preparations that received motoneuron and pTRG injections on opposite sides (D) or on the same side (E). The retrogradely labelled neurons shown on each illustrated section were sampled from three adjacent sections and pooled together into one. One section was skipped between each sampled section, to make sure that no cell was counted twice. This inevitably leads to an underestimation of the number of cells, but their distribution was the main interest. Double-labelled neurons appear in blue. The

grayed areas around the injection sites represent regions where analysis was impossible due to the high intensity of fluorescence (see B, C). The areas filled with green or magenta correspond to the area where the tissue was damaged by the pipette. Rectangles refer to the location of photomicrographs in B and C, and in Figure 1. The scale bars in B and C represent 200 μm. The scale bars in D and E represent 500 μm.
142x182mm (300 x 300 DPI)

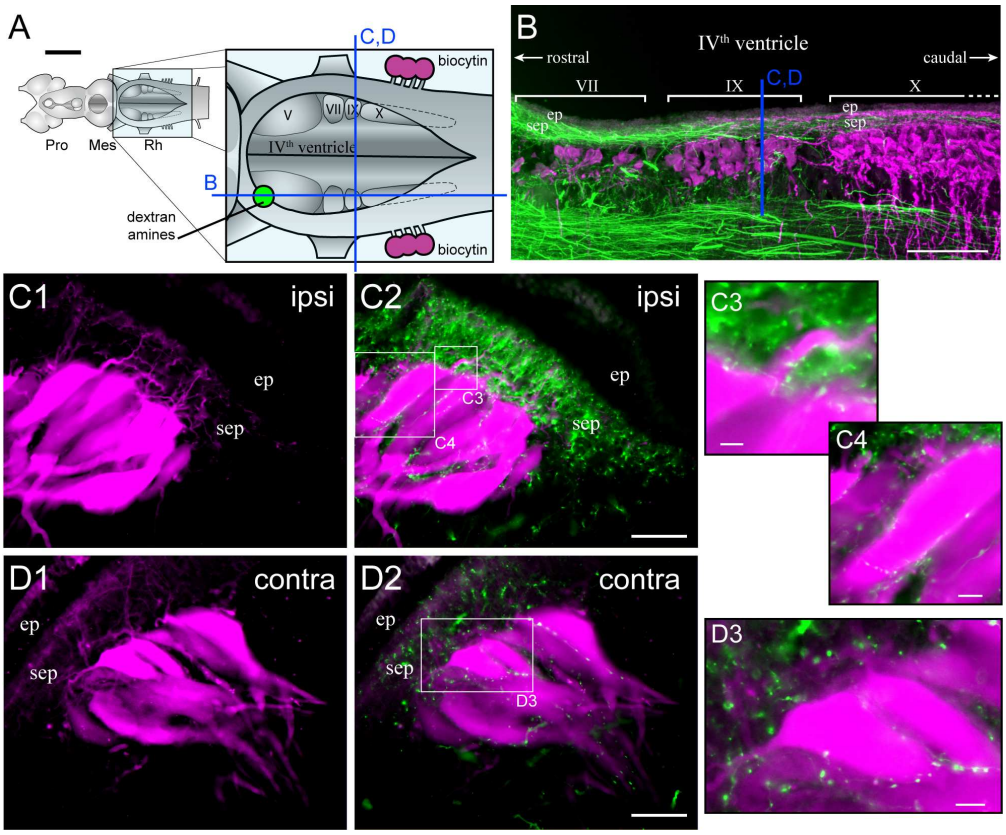

Projections from the pTRG area to respiratory motoneurons. A: Schematic representation of a dorsal view of the brain of the adult sea lamprey. To the right, the enlarged rhombencephalic region shows the location of the trigeminal (V), facial (VII), glossopharyngeal (IX) and vagal (X) motor nuclei at the bottom of the IVth ventricle. B: Photomicrograph of a parasagittal section through the respiratory motoneuron populations in a preparation that received a unilateral injection of FITC-dextran amines (green) into the pTRG. The motoneurons were labelled with biocytin (revealed in red with streptavidin-Alexa Fluor 594; displayed here in magenta) by injections of the three respiratory nerves peripherally. The illustrated section comes from the same side as the pTRG injection. Fibres from the pTRG area run longitudinally in the subependymal layer (sep) and in the tegmentum, ventral to the cell bodies of the motoneurons. Some of the fibres turn ventrally or dorsally to enter the motoneuron layer. C-D: High-power photomicrographs of glossopharyngeal respiratory motoneurons as they appear on cross sections. C1, D1: Motoneurons were clearly labelled on both sides of the brain (ipsi, ipsilateral, and contra, contralateral to the pTRG injection). Note the arborization of apical dendrites in the subependymal layer and basal dendrites in the tegmentum. C2, D2: Superimposed photomicrographs illustrating the proximity of fibres descending from the pTRG (green) and the dendrites and cell bodies of motoneurons. Elements in white are not double-labelled but result from the superimposition of the varicosities labelled from the pTRG that are in close proximity to the respiratory motoneurons. C3, C4, D3: The boxed area in C2 and D2 were enlarged to better show the green varicosities around motoneuronal elements. The scale bar in A represents 2 mm. B, 200 µm. C1, C2, D1, D2, 50 µm. C3, 5 µm. C4, D3, 10 µm. Pro: Prosencephalon, Mes: Mesencephalon, Rh: Rhombencephalon, V:Trigeminal motor nucleus, VII: Facial motor nucleus, IX: Glossopharyngeal motor nucleus, X: Vagal motor nucleus.
168x138mm (300 x 300 DPI)

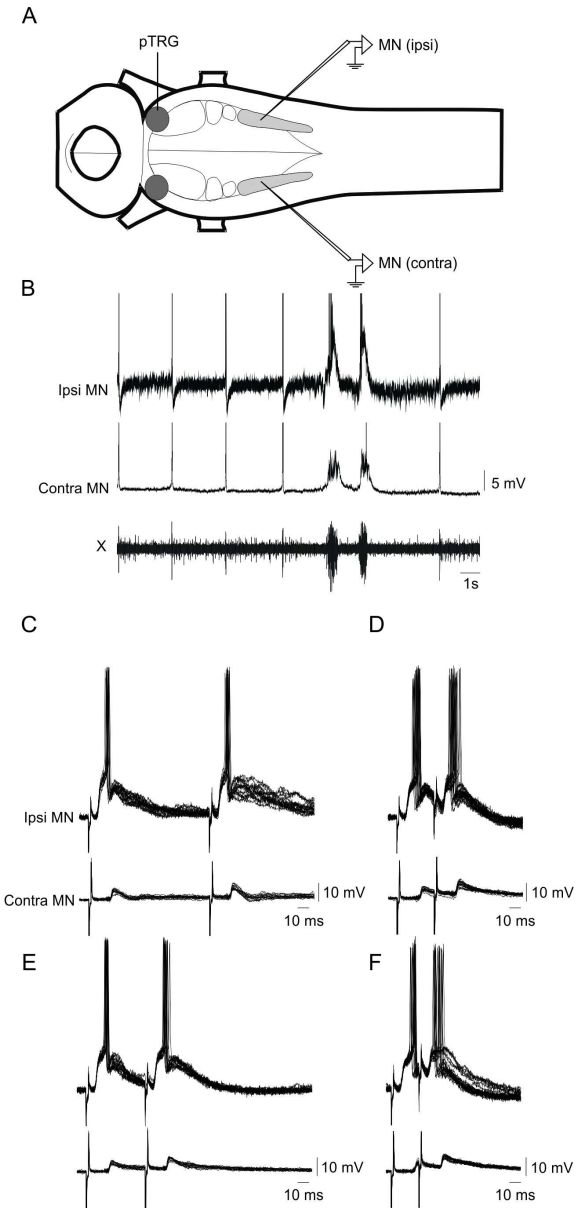

Characterization of bilateral descending inputs from the pTRG to pairs of simultaneously-recorded respiratory motoneurons on the two sides of the brainstem. A: Schematic representation of the lamprey brainstem. A respiratory motoneuron is recorded simultaneously from the two sides of the brain and a stimulating electrode is placed in the pTRG on one side. B: Recordings of spontaneous on-going fictive respiratory activity from a pair of motoneurons (MN) located on each side. The intracellularly-recorded respiratory bursts are in phase with those recorded extracellularly from the vagal motor nucleus (X). C-F: Intracellular excitatory responses to paired pulse stimulation with increasing frequency (C, D, E and F correspond to 10, 20, 30 and 40 Hz, respectively). pTRG: paratrigeminal respiratory group, MN: motoneuron, X: Vagal motor nucleus, ipsi: ipsilateral, contra: contralateral.
109x231mm (300 x 300 DPI)

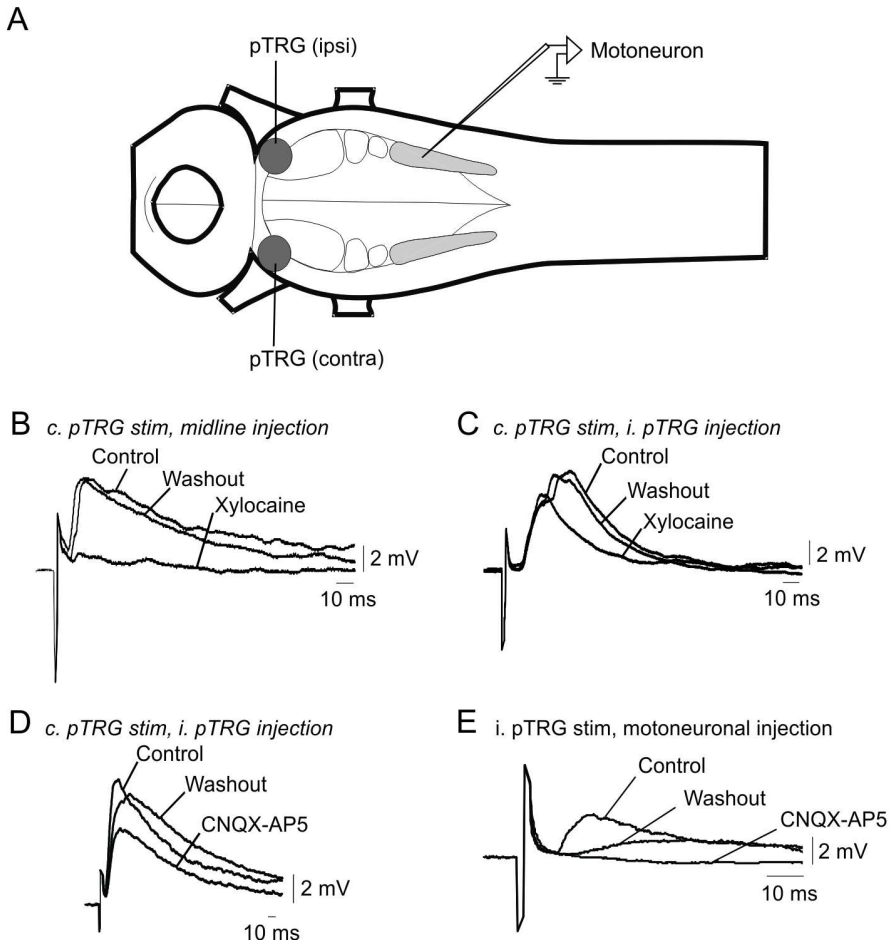

Electrophysiological characterization of the descending connections from the pTRG to the respiratory motoneurons. A: Schematic representation of the lamprey brainstem with the pTRG and respiratory motoneurons represented on both sides. B: Average of the EPSPs recorded from a respiratory motoneuron following electrical stimulation of the contralateral pTRG. Xylocaine was applied along the midline at the pTRG level. C: Average of the EPSPs recorded from a respiratory motoneuron following electrical stimulation of the contralateral pTRG. Xylocaine was applied in the ipsilateral pTRG. D: Average of the EPSPs recorded from a respiratory motoneuron following a stimulation of the contralateral pTRG. CNQX (1 mM) and AP-5 (500 µM) were applied in the ipsilateral pTRG. E: Intracellular recording of a respiratory motoneuron during stimulation of the ipsilateral pTRG. CNQX and AP-5 were injected directly over the recorded motoneuron. pTRG: paratrigeminal respiratory group, ipsi, i: ipsilateral, contra, c: contralateral.
135x126mm (300 x 300 DPI)

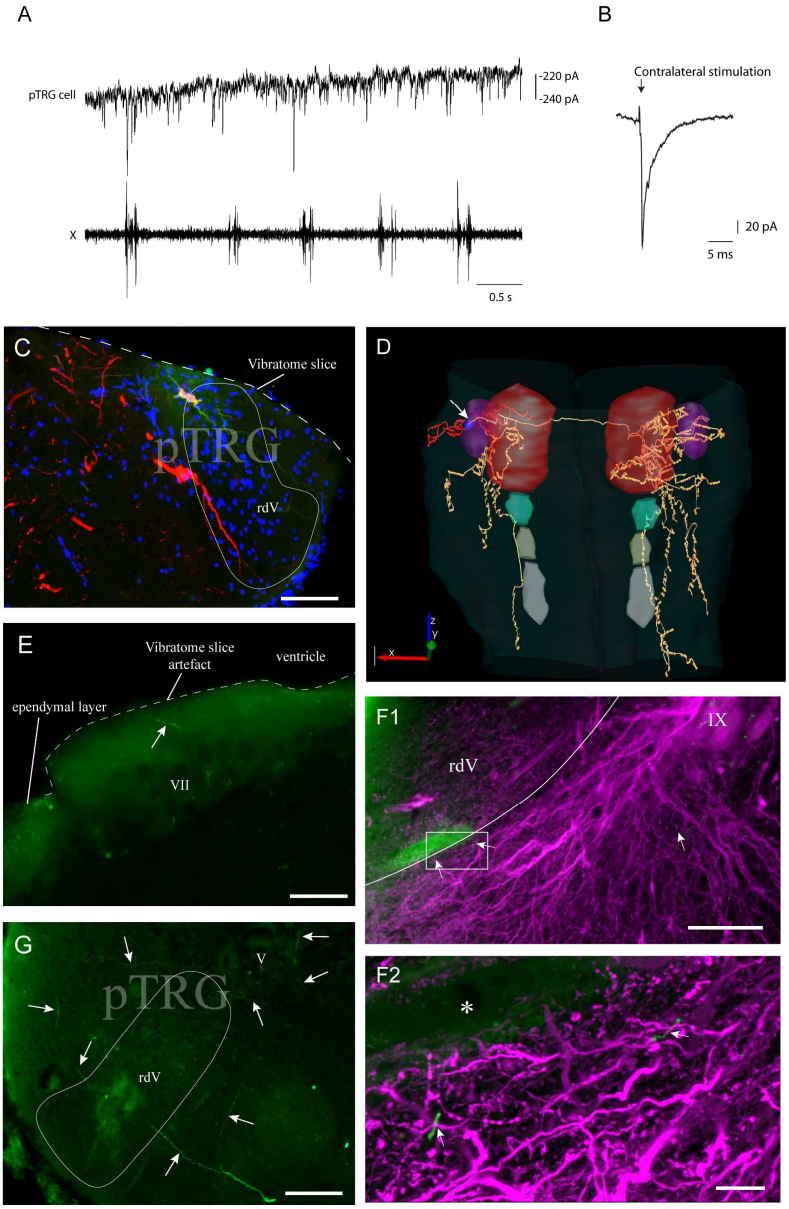

Electrophysiological and anatomical characterization of pTRG neurons. A: Patch recording of a pTRG neuron in whole-cell voltage-clamp mode. The neuron displays inward currents in phase with the respiratory activity recorded extracellularly from the vagal motor nucleus (X). B: Average of the inward currents induced by electrical stimulation of the contralateral pTRG. C: Superimposition of three photomicrographs of the recorded pTRG neuron filled with biocytin (green) and retrogradely-filled from an injection of dextran amines (red) in the X nucleus. DAPI labelling, in blue, shows the location of DNA-containing cell nuclei. D: 3D reconstruction of the axonal projections of the recorded pTRG neuron seen from a dorsal view of the rhombencephalon. Varicosities and dendritic spines are represented as circles. The diameter of the axons, dendrites and cell body (→) were amplified for better visibility. Dendrites, red arborizations; Soma, blue; Axons, yellow arborizations; V, red; VII, light blue; IX, light yellow; X, light gray; pTRG, purple. E: Photomicrograph illustrating axonal branches from the pTRG neuron innervating the ipsilateral facial motor nucleus (VII). F1: Photomicrograph illustrating axonal branches from the pTRG neuron around the dendrites of the IX

nucleus. The outlined area corresponds to the photograph in F2. F2: Z-projection of 14 adjacent optic slices (0.5 µm each) obtained from a confocal microscope. A larger diameter axonal branch with no varicosity (green, left arrow) and a smaller diameter axonal branch with varicosities (green, right arrow) were located in close proximity to the basal dendrites of the IX motoneurons (magenta) labelled from the tracer injection in the adjacent motoneuron pool. *, blood vessel. G: Photomicrograph illustrating axonal branches from the pTRG neuron innervating the contralateral pTRG. → indicates axonal branches. The scale bar in C represents 100 µm. D, the three axes represent 500 µm. E, 50 µm. G, 100 µm. F1, 100 µm. F2, 10 µm.
165x237mm (300 x 300 DPI)

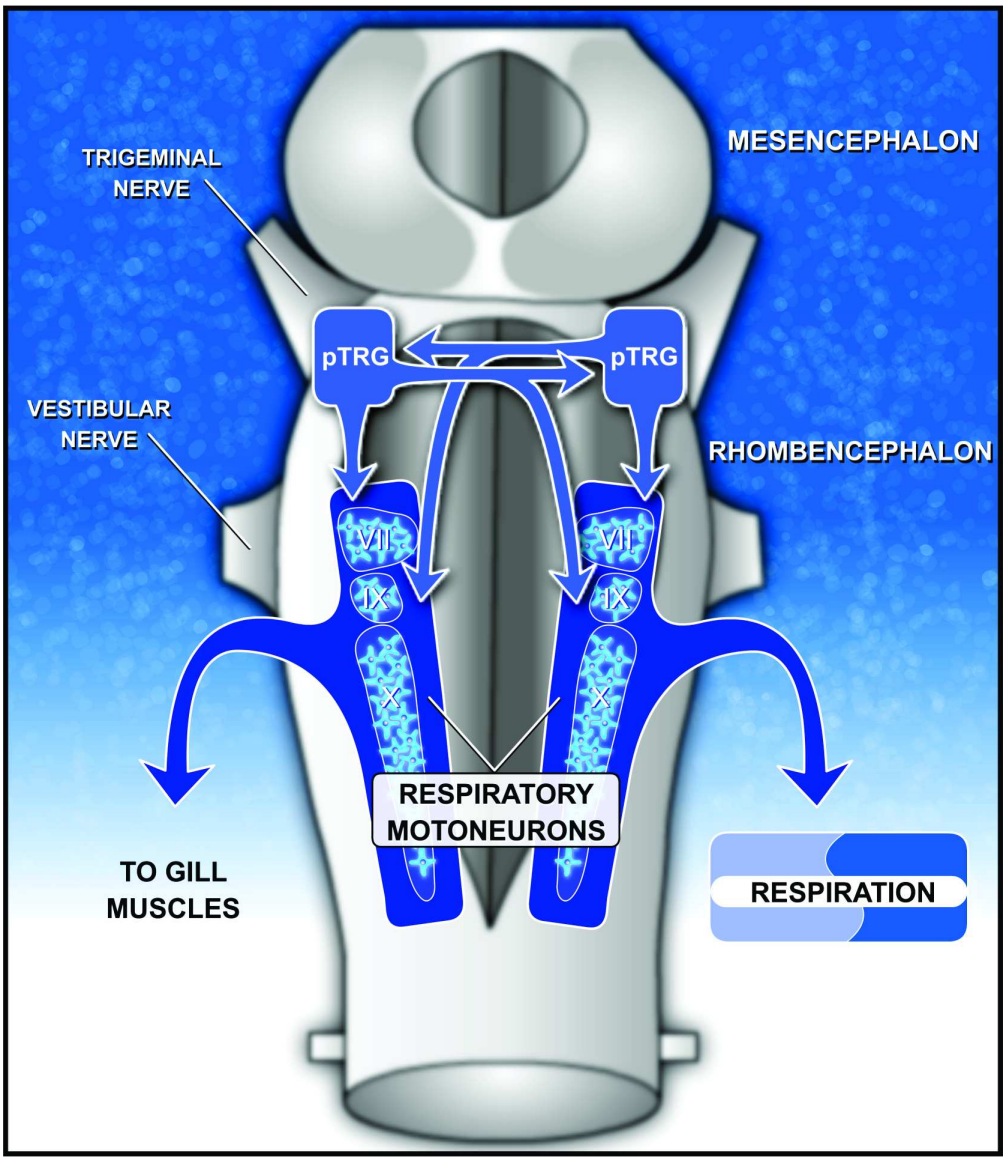

Schematic representation of the newly-identified connectivity in the respiratory networks of lampreys. Our study shows that neurons in the paratrigeminal respiratory group (pTRG), located in the rostral rhombencephalon, send axonal arborizations to the contralateral pTRG and bilaterally to the respiratory motoneurons. VII: facial nucleus, IX: glossopharyngeal nucleus, X: vagal nucleus.
141x162mm (300 x 300 DPI)

Neuron #	c. pTRG	iVII	iIX	iX	cVII	cIX	cX
01	√	√	√	√	√	√	√
02	√	√	√	√	√	√	√
03	√	√	√	√	√	√	√
04		√	√	√			
05	√				√	√	√
06	√	√	√	√	√	√	√
07	√	√	√	√	√	√	√
08	√	√	√	√	√	√	√